Using a spatially realistic load model to assess impacts of Alaskan glacier ice loss on sea level

Emma M. Hill,[1,2] James L. Davis,[1,3] Mark E. Tamisiea,[4] Rui M. Ponte,[5] and Nadya T. Vinogradova[5]

Received 3 March 2011; revised 7 July 2011; accepted 20 July 2011; published 20 October 2011.

[1] Ice loss from glaciers results in highly nonuniform patterns of sea level change due to the effects of self-attraction and loading. To quantify these spatial effects, it is necessary to obtain an ice load model that is both spatially realistic and regionally complete. We demonstrate a technique to produce such a model for the Alaskan glaciers by combining mass balance rates from a Gravity Recovery and Climate Experiment (GRACE) mascon solution with realistic glacier geometries. This load model can be used to solve the "sea level equation" to determine gravitationally self-consistent sea level and gravity rates. The model predicts a significant drop in relative sea level in the near field of the glaciers, with coastal rates of around −9 mm/yr (compared to a global average rise of 0.2 mm/yr) and significant differences to those predicted by a coarser model. The magnitude and sensitivity of these near-field rates imply that the near-field tide gauge records could contain significant information about the spatial distribution of ice loss. Comparison of model gravity rates with an independently produced, spherical harmonic, GRACE solution verifies that our technique can successfully capture the mass changes estimated in the mascon solution within our higher-resolution model. Finally, we use our ice load model to examine the possibility of detecting the effects of ice loss in estimates of ocean bottom pressure (OBP) from GRACE. We use the model to simulate the effects of GRACE signal leakage and show that the OBP signal from leakage has a similar pattern to, but larger amplitude than, the sea level "fingerprint" expected from ice loss.

Citation: Hill, E. M., J. L. Davis, M. E. Tamisiea, R. M. Ponte, and N. T. Vinogradova (2011), Using a spatially realistic load model to assess impacts of Alaskan glacier ice loss on sea level, *J. Geophys. Res.*, *116*, B10407, doi:10.1029/2011JB008339.

1. Introduction

[2] Recent studies have shown ice loss from Alaskan glaciers to be a significant component (~0.3 mm/yr) of global sea level rise [e.g., *Arendt et al.*, 2002; *Tamisiea et al.*, 2005; *Luthcke et al.*, 2008; *Berthier et al.*, 2010]. It has also been demonstrated that loss of ice from these glaciers will result in highly nonuniform patterns of sea level change due to the effects of gravitational self-attraction and loading, with each individual ice reservoir yielding a distinct spatial pattern of so-called "sea level fingerprints" [*Nakiboglu and Lambeck*, 1991; *Tamisiea et al.*, 2003]. Producing an accurate model for the glacier ice loss, and applying this model to predictions for spatial variations in the resulting sea level change, is therefore a vital piece of the climate change puzzle. It is also important to assess the level to which we are able to measure these sea level variations using the current geodetic observing system. Assessing the very near-field effects of glacier melting on sea level may provide the best chance of measuring the signal with the current system. Recent results have also illustrated the potential of ocean bottom pressure (OBP) measurements for studying the sea level signals at seasonal and longer timescales [*Tamisiea et al.*, 2010; *Vinogradova et al.*, 2010]. Thus, of particular interest is the question of whether it is possible to observe near-field effects in the estimates of OBP from the Gravity Recovery and Climate Experiment (GRACE) satellite mission.

[3] Achieving a suitable mass loss model for such sea level studies has, in the past, proven difficult. For example, in situ [e.g., *Dyurgerov*, 2002] and laser altimetry measurements [e.g., *Arendt et al.*, 2002, 2006, 2008] have high resolution in terms of measuring the mass balance for certain individual glaciers, but poor regional coverage (not all glaciers are measured) and often limited temporal resolution (e.g., *Arendt et al.* [2002] measure detailed profiles of recent ice thickness change along the length of 28 glaciers, for a period covering 5–7 years). Estimates obtained by differencing digital elevation models suffer from poor temporal resolution [*Larsen et al.*, 2007; *Berthier et al.*, 2010]. GRACE gravity

[1]Harvard-Smithsonian Center for Astrophysics, Cambridge, Massachusetts, USA.
[2]Also at Earth Observatory of Singapore, Nanyang Technological University, Singapore.
[3]Also at Lamont-Doherty Earth Observatory, Earth Institute at Columbia University, Palisades, New York, USA.
[4]National Oceanography Center, Liverpool, UK.
[5]Atmospheric and Environmental Research, Inc., Lexington, Massachusetts, USA.

Copyright 2011 by the American Geophysical Union.
0148-0227/11/2011JB008339

Table 1. Mascon Rates for the Period April 2003 to March 2007 From *Luthcke et al.* [2008] and Approximate Glacier Areas From the Digital Chart of the World Geometries

Mascon	Mascon Rate (Gt/yr)	Approximate Glacier Area (km^2)
01	−3.6 ± 0.3	4173
02	−4.2 ± 0.3	2720
03	−5.2 ± 0.4	2426
04	−4.8 ± 0.4	3679
05	−6.4 ± 0.4	8118
06	−8.2 ± 0.5	15196
07	−9.6 ± 0.6	22126
08	−4.8 ± 0.5	1598
09	−5.6 ± 0.5	1923
10	−12.9 ± 0.8	7787
11	−11.6 ± 0.7	9053
12	−7.4 ± 0.9	7417

measurements, on the other hand, can obtain good temporal resolution, continuous coverage, and a measurement of regional mass balance that does not suffer from "missing" glaciers [*Tamisiea et al.*, 2005; *Chen et al.*, 2006; *Luthcke et al.*, 2008]. However, systematic errors in the GRACE data have led to a requirement for smoothing and filtering, which reduces the spatial resolution [*Swenson and Wahr*, 2002, 2006] so direct estimation of individual glacier rates has not been possible. For studying the spatial effects of glacier ice loss on sea level, we require full regional coverage, but would like to have a more realistic spatial geometry for the ice mass changes. Here, therefore, we outline a technique to combine GRACE estimates of mass change (from a mass concentration, or "mascon," solution by *Luthcke et al.* [2008]) with glacier geometries, to produce an ice load model for the Gulf of Alaska that benefits from the continuous coverage of GRACE, but also has a more realistic spatial distribution.

[4] The spatially realistic ice load model has a number of useful applications. First, we use it to produce self-consistent estimates of sea level and gravity change due to ice mass change. We compare near-field estimates for relative sea level (RSL) change from our spatially realistic load with a model produced using the geometry of the mascon grid. We also compare the output gravity model with rates obtained using GRACE data processed independently and with a different representation (spherical harmonic expansion) from that used for the load model. This latter comparison not only allows us to validate our model load values, but also allows for consistent comparison of the spatial distribution of mass change from the two different GRACE solutions.

[5] Furthermore, we are able to assess the potential for observation of the near-field sea level effects in GRACE spherical harmonic solutions for OBP. Since the mass changes taking place on the continent are so much larger than the ocean effects, these solutions are likely to suffer from considerable "leakage" of the continental signal into the ocean, as a result of the low spatial resolution. Techniques have been developed to mask the continental signals, in order that OBP signals can be assessed [*Wahr et al.*, 1998]. These techniques, however, are unlikely to remove all the leakage effects [*Chambers et al.*, 2007; *Chambers*, 2009; *Quinn and Ponte*, 2010]. In this study we convert our spatially realistic ice load model to spherical harmonic gravity coefficients, in order to simulate the continental mass change as "seen" by GRACE (which will measure both this and the sea level effects). We are then able to test the masking algorithm on our ice load model to determine the extent of the remaining leakage signal over the ocean area close to the glaciers. Comparison of this with masked GRACE results and a model for the expected sea level fingerprint in OBP illustrate that care must be taken when interpreting near-coastal OBP rates from GRACE.

[6] We note that although this model is "spatially realistic" in the context of our specified goal of sea level studies, we make a number of assumptions that do not render it so in the context of glaciological studies. We refrain, therefore, from making glaciological interpretations of our results. Some of the results of this study, however, indicate that a more detailed study, with a goal of examining the spatial details of glacier mass loss through the resulting self-attraction and loading signals, may be warranted.

2. Input Data for the Ice Load Model

[7] Our goal is to assign the mass change rates (Table 1) from the GRACE mascon solution of *Luthcke et al.* [2008] to the correct geometry of the glaciers (Figure 1). In this section we describe these data sets in more detail.

[8] *Luthcke et al.* [2008] provide rates of mass change for the Alaska glaciated region obtained by processing the GRACE Level-1 data with a parameterization of local mass variations as surface mass concentrations ("mascons") [*Rowlands et al.*, 2002; *Luthcke et al.*, 2006; *Rowlands et al.*, 2010]. An overview of the historical development of the theory of mascons, and comparison with the spherical harmonic approach to representing a gravity field, is discussed by *Werner and Scheeres* [1997]. Unlike solutions produced using spherical harmonic expansion of Level-2 data coefficients, local GRACE mascon solutions allow for spatial and temporal constraints, enabling estimation of mass variations at a higher spatial and temporal sampling frequency. Each mascon (Figure 1) covers a 2° × 2° grid square. *Arendt et al.* [2008] performed a validation of these mascon rates for the St. Elias mountains using aircraft laser altimetry measurements, indicating good agreement between the two techniques.

[9] The mascon rates for total mass loss compare favorably with previous studies that utilize the alternative GRACE processing approach of global spherical harmonic decomposition [*Tamisiea et al.*, 2005; *Chen et al.*, 2006]. For the period of April 2003 to March 2006, *Luthcke et al.* [2008] estimate a rate of −102.1 ± 5.2 Gt/yr, while *Tamisiea et al.* [2005] estimate a rate of −110 ± 30 Gt/yr and *Chen et al.* [2006] estimate −101 ± 22 Gt/yr (although they analyze slightly shorter time spans, which limits the significance of this comparison because rates calculated using different time periods can vary significantly). The solution by *Luthcke et al.* [2008] also agrees well with estimates of mass balance obtained from laser altimetry (total extrapolated mass loss of −96 ± 35 Gt/yr) for the period from the mid-1990s to 2000–2001 [*Arendt et al.*, 2002].

[10] For our model input we use the mascon rates by *Luthcke et al.* [2008] for April 2003 to March 2007, which have a total mass loss rate of −84.2 ± 5.0 Gt/yr. By interpreting these rates as reflecting the glacier mass balance we assume that all non glacier sources of mass variation have

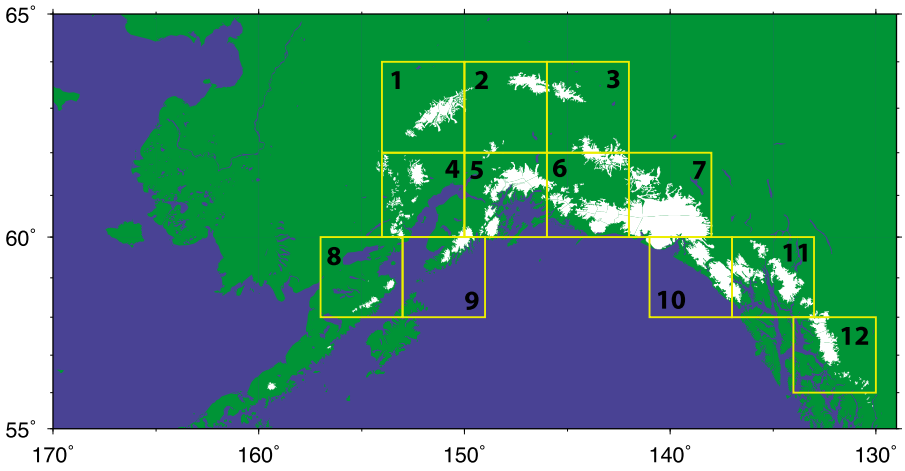

Figure 1. Glaciated regions (displayed in white) from the Digital Chart of the World, and mascon definitions from *Luthcke et al.* [2008] (yellow boxes) for the Alaska region.

been accounted for in the forward modeling done by *Luthcke et al.* [2008], and therefore that all mass loss from a mascon region should be attributed to glacier ice loss. The forward modeling includes ocean tides, atmospheric gravity, a barotropic ocean model, changes in terrestrial water storage, and glacial isostatic adjustment (GIA) (both ICE-5G [*Peltier*, 2004] and a model for the Little Ice Age [*Larsen et al.*, 2005]). It does not include tectonic effects. It is therefore possible that mascons 4–6 and 8–9 may be affected by postseismic deformation following the M_w 9.2 1964 Alaska earthquake [*Zweck et al.*, 2002; *Suito and Freymueller*, 2009], while estimates for mascons 2 and 3 may have been affected by the 2002 M 7.9 Denali Fault earthquake [*Freed et al.*, 2006; *Johnson et al.*, 2009].

[11] We use polygons representing glacier geometry (Figure 1) from the Digital Chart of the World (DCW), with the primary source being the U.S. Defense Mapping Agency Operational Navigation Chart series. We downloaded the geometries as a compilation of DCW tiles for Alaska from http://www.asgdc.state.ak.us. The accuracy of these geometries is limited, since they were obtained by digitization of historic maps, but at the time of writing they represent the only complete inventory of glaciers for this region. We assume these geometries to be constant in time, and assume that all glaciers within an individual mascon square will have the same rates of mass loss. For our purposes in creating a load model for sea level studies, these inaccuracies and assumptions should not be too significant, but it should be clear that when we refer to these geometries and our load model as "spatially realistic," we do so in the context of our sea level study, not for glaciological interpretation. Our comparison of sea level results (section 4.2) using the mascon and refined geometries gives some indication of the sensitivity of our model to these inaccuracies.

3. Method

[12] To study the spatial effects on sea level of ice mass loss, an ice load is applied to the "sea level equation" (SLE) [*Farrell and Clark*, 1976; *Mitrovica and Peltier*, 1991]. Solution of the SLE results in gravitationally self-consistent RSL rates that account for deformation of the solid Earth and perturbation of the geoid due to an applied load (ocean plus ice). The assumption is that all mass lost from the glaciers goes into the ocean and is redistributed taking into account the effects of self-gravitation and loading. Since we consider only contemporary load changes, we disregard the viscoelastic terms in the Green's functions and consider only the elastic response. Love numbers were calculated using the Preliminary Reference Earth Model [*Dziewonski and Anderson*, 1981] and the expansion performed up to degree and order 512. We output the predicted geoid changes as spherical harmonic coefficients. We also output, for our analysis of leakage effects, the spherical harmonic coefficients for the ice-only (input) load model.

[13] To create this ice load we first create masks for both mascon and glacier geometries. Masks are created on a Gauss-Neumann grid [*Sneeuw*, 1994] to aid spectral decomposition. We then assign ice thickness rates, $\dot{h}_k$, to the glacier mask using the mascon rates, via the equation

$$\dot{h}_k = \frac{\dot{m}_k}{\rho_i A_k} \tag{1}$$

where $\dot{m}_k$ is the mascon rate, ρ_i is the density of ice and A_k is the area of the glaciers within the kth mascon (calculated using the input glacier geometries). We also calculate ice thickness uncertainties by applying the mascon uncertainties from *Luthcke et al.* [2008] to this equation in place of $\dot{m}_k$.

[14] We use a value of 900 kg/m^3 for ice density. The true density is likely to vary considerably within the region, but we do not have the data or models to determine more appropriate values (see discussion by *Arendt et al.* [2008]). Since the goal of assigning the mass loss to glacier geometries is to derive the following sea level calculations, the introduction of density is not strictly necessary. However, conversion of the values to ice thickness provides for intuitive interpretation of the results.

4. Results and Discussion

[15] Here we present a brief description of the ice load model produced using our technique. We next present a comparison of our output model for RSL with a model

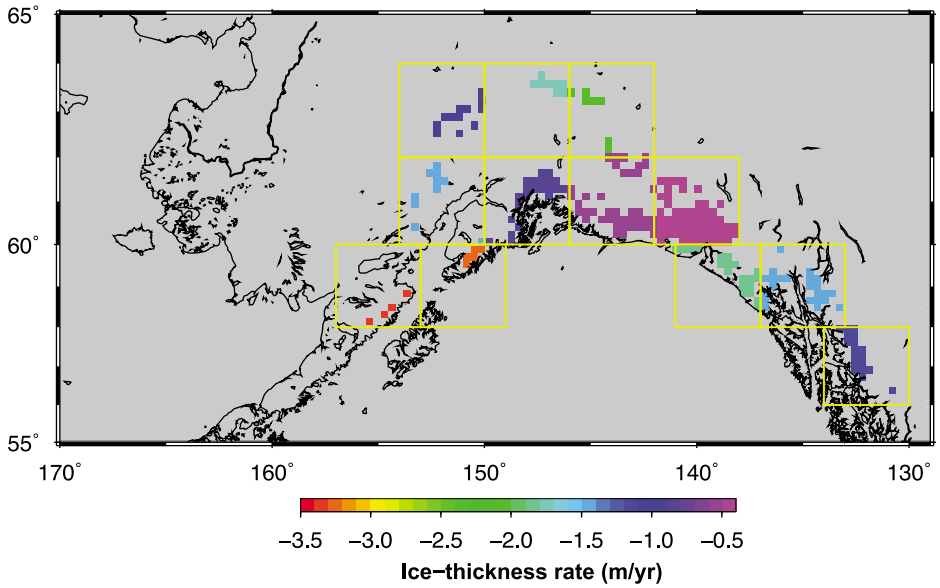

Figure 2. Ice load model depicted as ice thickness rates, calculated using procedure described in text. Yellow boxes indicate mascon definitions from *Luthcke et al.* [2008].

produced using the mascon geometries, and a comparison of our output gravity model with independently processed GRACE results. Finally, we discuss use of these models to assess the effects of signal leakage on near–coastal OBP rates from GRACE.

4.1. Ice Load Model

[16] We present ice thickness rates to illustrate the effects of normalizing the GRACE mass loss to glacier area. As previously stated, although these results are of significant utility for sea level studies, they are not designed for glaciological interpretation, due to the assumptions (e.g., use of uniform ice density) listed in section 2. We therefore quote only approximate numbers for thickness change.

[17] The mascon rates show the greatest mass losses for the southeast mascons (numbers 7, 10, and 11 in Figure 1). Since the ice thickness rates also take into account glacier area (Table 1), however, these are not the regions with the highest ice thickness rates (Figure 2). For example, the high level of glacial coverage in mascon 7, which contains a large part of the St. Elias range, leads to a relatively low (compared to other mascons) ice thickness rate of <1 m/yr, despite the high rates of mass loss. Conversely, some areas with lower rates of mass loss have high rates of ice thickness change due to their limited glacial coverage. For example, mascon 9, which covers the majority of the Harding Icefield, has an estimated ice thickness rate of ~3 m/yr, which is necessary to reconcile the mascon solution with the small glacier area.

4.2. Relative Sea Level Results

[18] To assess the value in converting the GRACE mass loss rates to spatially realistic geometries we compute RSL rates using both an ice load with the geometries of the mascon grid squares (Figure 3a) and our ice load with realistic glacier geometries (Figure 3b). The mascon and glacier geometries are shown in Figure 1.

[19] As a result of the glacial unloading, the solid surface in the near field of the glaciers will rebound. Simultaneously, there will be a drop in the near-field sea surface as water flows away from the area, because of the reduced gravitational attraction to the glacier mass. Therefore, although the eustatic global sea level rise associated with our model is 0.2 mm/yr, the Gulf of Alaska sees a significant drop in RSL, with negative rates in the very near field of the glaciers of ≥9 mm/yr predicted by our spatially realistic model.

[20] The use of a spatially realistic load model will not have a large impact on the modeled global pattern of sea level rise. However, it does have regional consequences, as seen in Figure 3. For example, at a point on the coast near the area of highest mass loss (coordinates 137.8°W, 58.7°N) we estimate a sea level drop of −6.8 mm/yr for the mascon geometries, and −8.8 mm/yr using realistic geometries. This difference of 2.0 mm/yr is due to the fact that the sea level drop is more concentrated close to the glaciers for the high-resolution study, while the signal for the mascon geometries has a broader, lower-amplitude peak. These rates are clearly large enough to be of significant importance for studies using the regional tide gauge network. For example, investigations of regional tectonic uplift using tide gauge data have tended not to include these effects [e.g., *Larsen et al.*, 2003].

4.3. GRACE Comparison

[21] The spherical harmonic and mascon approaches to processing GRACE data have independent strengths and weaknesses [e.g., *Werner and Scheeres*, 1997], and relatively few self-consistent comparison studies exist. An example of such a comparison, for global fields, has been performed by *Rowlands et al.* [2010]. Our technique for producing a load model affords us a useful opportunity to compare the mascon solution with a solution using Stoke's coefficients, as well as verify our model against an independent solution.

[22] For the independent analysis of the GRACE data we use rates from a global spherical harmonic solution based on the University of Texas at Austin Center for Space Research (UTCSR) Release-04, Level-2, data set. The spherical harmonic expansion was performed up to degree and order

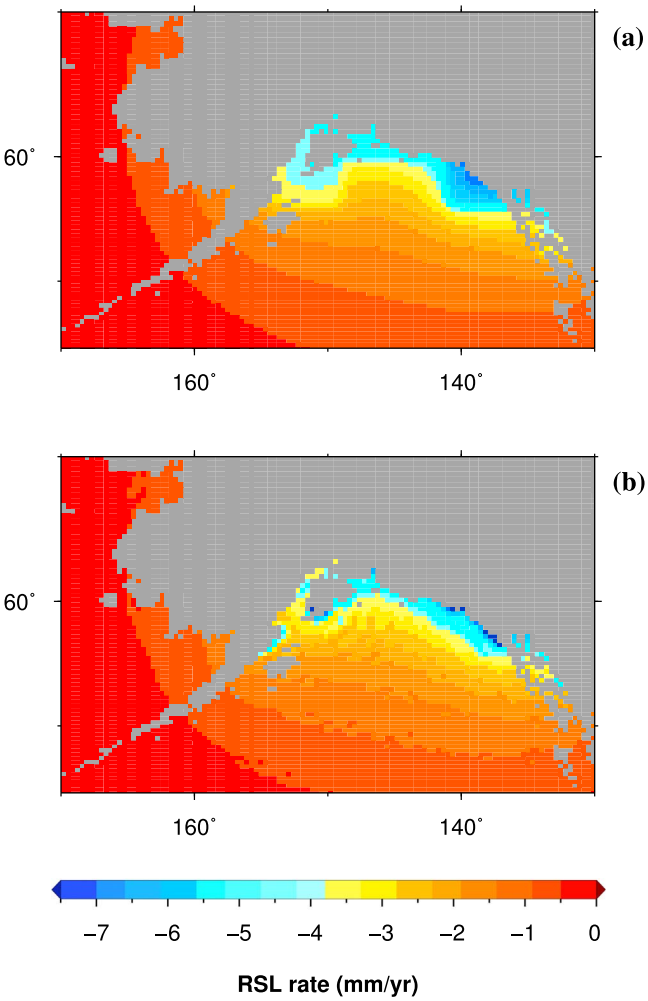

Figure 3. Relative sea level rates predicted by our model using (a) ice load with mascon geometries (grid squares) and (b) ice load with realistic glacier geometries. Spherical harmonic expansion was to degree and order 512. The color bar was selected to highlight the spatial variability. It saturates to more negative numbers very close to the coast (darkest blue) for the model with realistic geometries.

60, and estimated rate coefficients were smoothed using a Gaussian filter of 500 km width [*Wahr et al.*, 1998]. We use the same time span as used for the mascon solution. The rates were corrected for ongoing GIA using a model based on the ICE-5G ice model and VM2 Earth model [*Peltier*, 2004]. The prediction utilized the sea level theory collected by *Kendall et al.* [2005], and the rotational theory of *Mitrovica et al.* [2005]. The UTCSR Level-2 coefficients have an ocean and atmosphere model removed, so we added this model back into the solution (using the global area coverage coefficients from UTCSR) so that ocean effects are included. We did not correct for changes in terrestrial water storage, as discussed below. Correlated signals in the GRACE data that cause north-south stripes were removed as suggested by *Swenson and Wahr* [2006].

[23] For comparison with the GRACE spherical harmonic solution, we expanded the spherical harmonic gravity change coefficients from our model output from the SLE (with our realistic ice load applied) to degree and order 60, and smoothed this field with a 500 km width Gaussian filter. Spatial smoothing of the GRACE data will reduce signal amplitude over the small area covered by the Alaskan glaciers [*Tamisiea et al.*, 2005]. We do not estimate and apply a scaling factor to account for this, so while we can now consistently compare the amplitudes and spatial distributions of the GRACE and model rates, they do not represent the "true" amplitudes of total mass loss. However, the "true" amplitudes should be more closely reflected by the high-resolution ice model.

[24] Figure 4 shows rates from both the GRACE spherical harmonic solution and the output model results (ocean plus ice). The largest differences are outside the glaciated region (Figure 5). Within the glaciated region the two solutions have good agreement. Peak signals for the model and GRACE

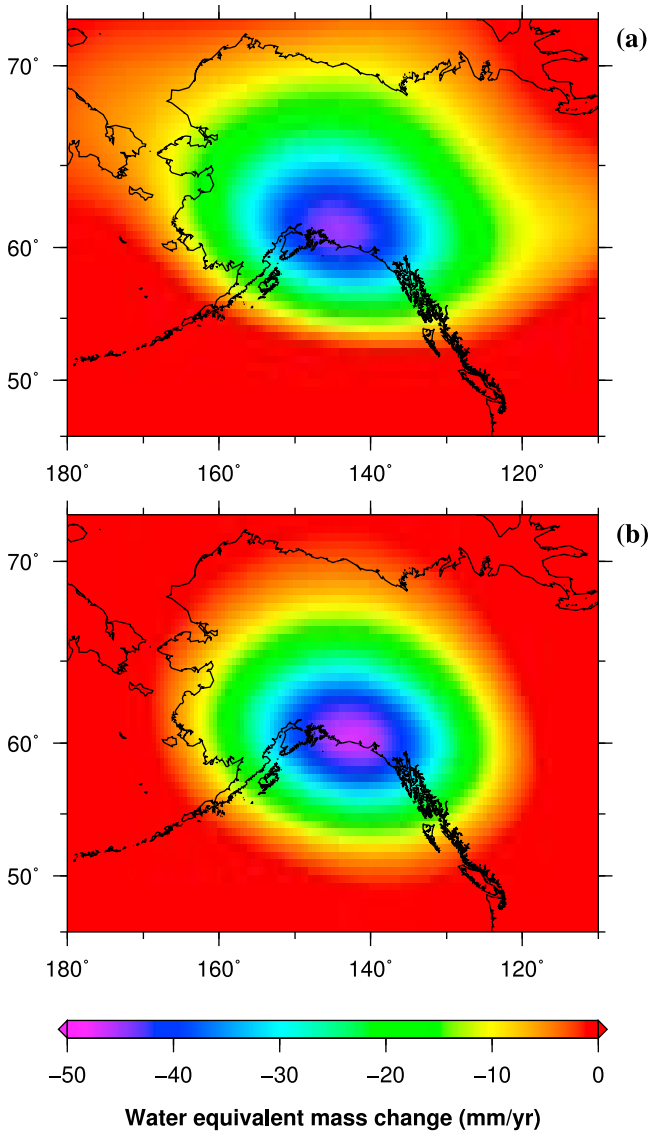

Figure 4. Mass change rates from (a) the GRACE spherical harmonic solution and (b) our model (ocean plus ice), both smoothed with a 500 km Gaussian filter and truncated at degree 60.

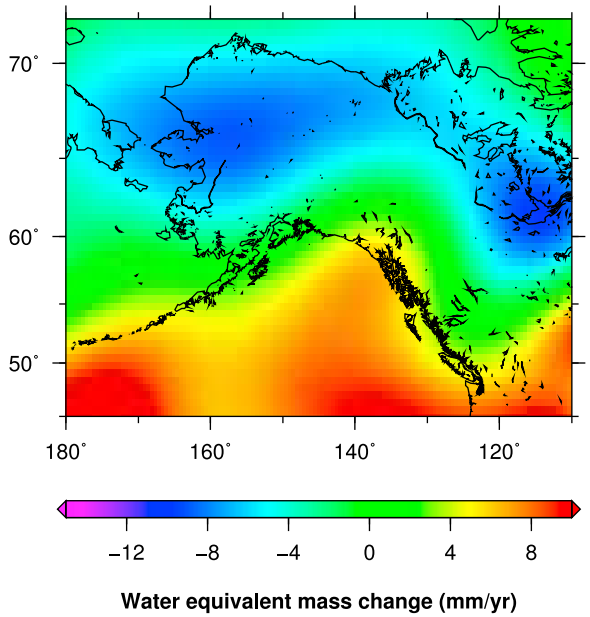

Figure 5. Difference between the GRACE spherical harmonic solution (Figure 4a) and our model (Figure 4b).

results are −47 ± 2 mm/yr and −45 ± 1 mm/yr, respectively. Possible explanations for the differences in two solutions are discussed below. Model uncertainties were calculated using a Monte Carlo technique, in which we computed the ice load model using mascon rates with Gaussian noise added that had a standard deviation corresponding to the mascon uncertainties. We then solved the SLE. This was repeated with 3500 iterations and the 95% confidence interval assessed. These error bars do not, therefore, include uncertainties due to some of the simplifications discussed in section 4.1.

[25] *Luthcke et al.* [2008] show that their terrestrial water storage (TWS) model (based on the Global Land Data Assimilation System/Noah, but with TWS contribution in glaciated areas set to zero) is inconsistent with the Alaska mascon rates. They conclude that this is not a problem for the mascon solution, since their tests indicate that any contribution to the glacier mascons from TWS in the surrounding area is small relative to the glacier mass change. However, this inconsistency could be a problem for our spherical harmonic solution, in that truncation and smoothing will result in leakage from this inconsistent TWS model into the glaciated region. Since the actual TWS rates are likely to be very small [*Luthcke et al.*, 2008] we do not remove a TWS model from the spherical harmonic solution. Hydrological effects from inland Alaska may, therefore, leak into our GRACE spherical harmonic solution in the glaciated region, causing small inconsistencies with the mascon solution. We also did not account for the viscous response to post–Little Ice Age GIA following the collapse of the Glacier Bay Icefield [*Larsen et al.*, 2005] in the spherical harmonic solution, whereas this was accounted for in the mascon solution. This omission could also partly account for the difference we see in the glaciated area. The magnitude of this signal is expected to be ~7 Gt/yr, with a ±30% error [*Luthcke et al.*, 2008] (compared to a total mass loss of −84.2 ± 5.0 Gt/yr for the mascon solution).

4.4. GRACE Masking and Signal Leakage

[26] The difference between the ice-only gravity model (based on our high-resolution ice load) and the full output gravity model (output from the SLE, so includes gravitationally self-consistent estimates of both ice and ocean effects) will reflect the ocean part of the signal (i.e., the sea level fingerprint in OBP as would be measured by GRACE). This is shown in Figure 6. The minimum rate, in units of equivalent water thickness, is −1.1 mm/yr (with no attempt made to rescale the results after smoothing).This signal is, clearly, considerably smaller than the signal from the ice mass change itself. The full model (Figure 4b) and ice-only model (not shown) are almost identical. Thus, removal of the ice-only load from the GRACE data produces a picture similar to Figure 5. Clearly, noise in the GRACE data could overwhelm this very small sea level fingerprint.

[27] The fact that the ice load is so large compared to the ocean component also raises the question of whether leakage effects in the GRACE results will overwhelm any trace of a sea level fingerprint. Previous studies have recognized the problem of continental leakage, where the land signals are so great they significantly contaminate the ocean signals as a result of the smoothing and truncation, and have suggested that the problem can be reduced by a process of continental masking [e.g., *Wahr et al.*, 1998]. Since we now have a high-resolution model for the gravity signal coming only from the continents, we can test the effectiveness of this masking.

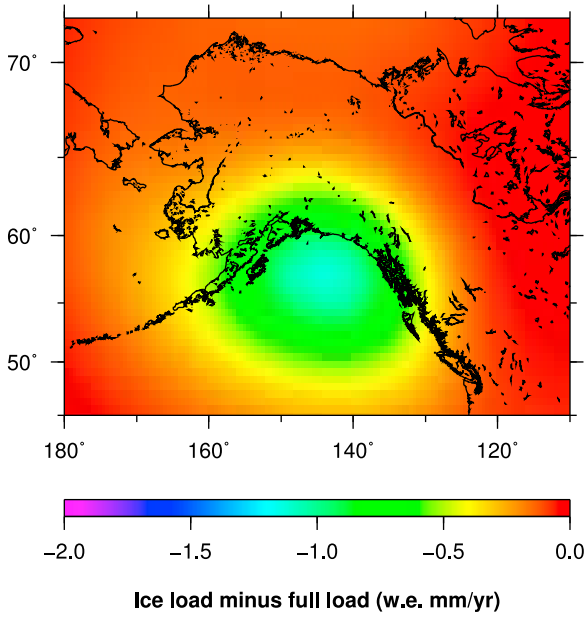

Figure 6. Difference between the full (ice and ocean) and ice-only loads, which have been converted to spherical harmonic gravity coefficients and reconstructed to a grid of rates (in values of equivalent water thickness) with our GRACE processing routine, which includes 500 km Gaussian smoothing. This illustrates the magnitude of the sea level fingerprint we would expect to observe in our GRACE spherical harmonic solution. Note that the color scale is considerably smaller than for Figure 5.

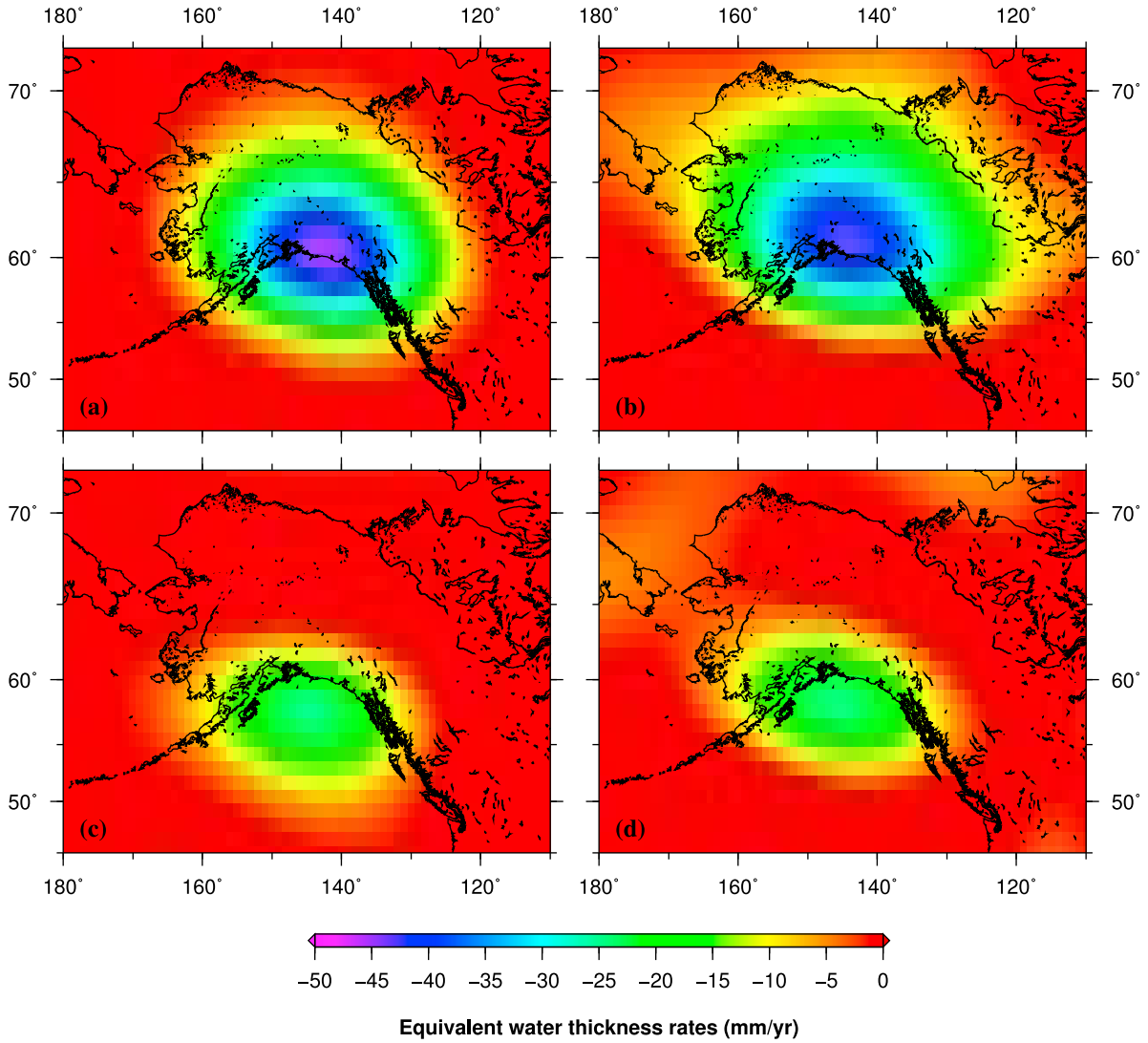

Figure 7. Unmasked mass change rates from (a) the ice–only load model and (b) GRACE and (c and d) corresponding mass change rates after applying a continental mask (i.e., the effects of signal leakage from the continents into the ocean). All fields were smoothed with a 500 km Gaussian filter. The effect of leakage causes an erroneous sea level "fingerprint," which is considerably larger than that estimated from our models (Figure 6).

[28] We follow the methodology outlined by D. P. Chambers (Converting Release-04 gravity coefficients into maps of equivalent water thickness, unpublished report, 9 pp., 2007, available at http://grace.jpl.nasa.gov/files/GRACE-dpc200711_RL04.pdf, hereinafter referred to as Chambers, unpublished report, 2007) to perform continental masking of both the ice load and GRACE data. We first reconstruct a gridded data set from the spherical harmonic coefficients, without the use of smoothing parameters. We truncate both solutions to degree and order 64. (GRACE UTCSR data is only available to degree 60, but the Gauss-Neumann grid we use for decomposing back to spherical harmonics requires a maximum degree that is a power of 2. Degrees 61–64 for the GRACE data are therefore empty here.) We next mask the oceans from both grids to get a "land only" solution. We decompose the masked grid back to spherical harmonic coefficients and run these through our regular GRACE processing code, which includes Gaussian smoothing with a 500 km radius, to get values for equivalent water thickness (land only). Finally, we subtract the land-only solution from the full solution, which is also processed with a 500 km smoothing radius, to get values that should cover only the oceans. Better masking results can be achieved by extending the mask some distance away from the coastlines, to correspond with the width of the filter (e.g., Chambers, unpublished report, 2007). We do not do this since it is the near-coast signals that we are interested in investigating.

[29] Figure 7 shows the results with and without the continental mask applied. Continental masking clearly reduces the amplitude of the leaked signal over the oceans in both the ice load and GRACE results (compare signal over the ocean in Figures 7a and 7c (model), and Figures 7b and 7d (GRACE)). However, signal over the ocean remains, with similar patterns to our model fingerprint (Figure 6) but significantly larger amplitudes (minimum signal of −26 mm/yr water equivalent

for the ice load model and −30 mm/yr for GRACE, compared to −1 mm/yr for the model fingerprint). Since the ice load model represents only mass change occurring on the land, we know that it should not contain a sea level fingerprint. This therefore illustrates that great care must be taken in interpreting signals in the GRACE OBP results, particularly for areas close to the continents, that give the appearance of a sea level fingerprint.

5. Conclusions

[30] We have presented a technique to combine GRACE estimates of mass loss with glacier geometries. While not accurate enough for glaciological studies, the resulting load model represents a significant step toward understanding the effects of ice loss on sea level.

[31] Application of our load model to the SLE allows us to calculate self–consistent sea level and gravity rates for the local area. The use of a spatially realistic load model produces significantly different estimates for sea level change to those produced using a load model based on the mascon grid, with differences at the level of ≥2 mm/yr. We estimate rates of sea level drop of up to ~9 mm/yr. Rates of this magnitude, and the demonstrated variation in rates between results from the different load models, should be significant for studies analyzing the regional tide gauge data for sea level or tectonic rates. In particular, the sensitivity of the near-field rates suggests that near–field tide gauge records can contain significant information about the spatial distribution of ice mass loss, at this and other glaciated regions. Attempts to detect these signals using near-field tide gauges (and also GPS or, potentially, seafloor geodesy) will require more accurate representation of the glacier geometries and mass changes than we use in this paper, and consideration of a number of additional processes such as tectonic deformation, but this first-order evaluation of the potential magnitude of the signals suggests it would be an effort worth making.

[32] We also calculate self-consistent gravity rates using our load model and the SLE. We compare these to an independent GRACE solution that uses spherical harmonic expansion. This provides a consistent way to compare gravity changes estimated by the two different (spherical harmonic and mascon) GRACE solutions, and our results indicate that the two solutions agree reasonably well for the glaciated region, with various explanations for differences between the solution. Good agreement between the model and GRACE spherical harmonic solution also verifies that our technique is successfully able to capture the mass changes estimated in the GRACE mascon solution within our higher-resolution model.

[33] Compared to the magnitude of the ice load, the corresponding sea level fingerprint in OBP is very small. We show that it would be difficult to discern such a signal in a GRACE OBP solution processed using a regular spherical harmonic expansion with Gaussian smoothing. We also show that care must be taken in interpreting signals in the GRACE OBP solution for areas close to the continents. Indeed, we use the ice load model to simulate the effects of signal leakage in the GRACE solution, and show that these effects have a very similar pattern to the sea level fingerprint that we might expect from ice loss.

[34] **Acknowledgments.** This work was supported by NASA grants NNX08AJ79G, NNX07AM77G, NNX11AC14G, and NNX11AB97G. E. M. H. was partially supported by the Earth Observatory of Singapore (EOS number 32). M.E.T. was funded by NERC as part of Oceans 2025. We are grateful to Scott Luthcke for providing the bounding box coordinates for his published mascon results and to Katherine Quinn for useful discussions. Our routine uses the Generic Mapping Tools [*Wessel and Smith*, 1998]. The manuscript was significantly improved by reviews from Chris Larsen, two anonymous reviewers, and the Associate Editor.

References

Arendt, A. A., K. A. Echelmeyer, W. D. Harrison, C. S. Lingle, and V. B. Valentine (2002), Rapid wastage of Alaska glaciers and their contribution to rising sea level, *Science*, *297*, 382–386.

Arendt, A. A., K. A. Echelmeyer, W. D. Harrison, C. S. Lingle, S. Zirnheld, V. B. Valentine, B. Ritchie, and M. Druckenmiller (2006), Updated estimates of glacier volume changes in the western Chugach Mountains, Alaska, and a comparison of regional extrapolation methods, *J. Geophys. Res.*, *111*, F03019, doi:10.1029/2005JF000436.

Arendt, A. A., S. B. Luthcke, C. F. Larsen, W. Abdalati, W. B. Krabill, and M. J. Beedle (2008), Validation of high-resolution GRACE mascon estimates of glacier mass changes in the St Elias Mountains, Alaska, USA, using aircraft laser altimetry, *J. Glaciol.*, *54*(188), 778–787.

Berthier, E., E. Schiefer, G. K. C. Clarke, B. Menounos, and F. Remy (2010), Contribution of Alaskan glaciers to sea-level rise derived from satellite imagery, *Nat. Geosci.*, *3*, 92–95, doi:10.1038/NGEO737.

Chambers, D. P. (2009), Calculating trends from GRACE in the presence of large changes in continental ice storage and ocean mass, *Geophys. J. Int.*, *176*, 415–419, doi:10.1111/j.1365-246X.2008.04012.x.

Chambers, D. P., M. E. Tamisiea, R. S. Nerem, and J. C. Ries (2007), Effects of ice melting on GRACE observations of ocean mass trends, *Geophys. Res. Lett.*, *34*, L05610, doi:10.1029/2006GL029171.

Chen, J. L., B. D. Tapley, and C. R. Wilson (2006), Alaskan mountain glacial melting observed by satellite gravimetry, *Earth Planet. Sci. Lett.*, *248*, 368–378.

Dyurgerov, M. (2002), Glacier mass balance and regime: Data of measurements and analyis, 1945–2003, http://nsidc.org/data/g10002.html, Natl. Snow and Ice Data Cent., Boulder, Colo.

Dziewonski, A. M., and D. L. Anderson (1981), Preliminary reference Earth model, *Phys. Earth Planet. Inter.*, *25*, 297–356.

Farrell, W. E., and J. A. Clark (1976), On postglacial sea level, *Geophys. J. R. Astron. Soc.*, *46*, 647–667.

Freed, A. F., R. Bürgmann, E. Calais, J. Freymueller, and S. Hreinsdóttir (2006), Implications of deformation following the 2002 Denali, Alaska, earthquake for postseismic relaxation processes and lithospheric rheology, *J. Geophys. Res.*, *111*, B01401, doi:10.1029/2005JB003894.

Johnson, K. M., R. Bürgmann, and J. T. Freymueller (2009), Coupled afterslip and viscoelastic flow following the 2002 Denali Fault, Alaska earthquake, *Geophys. J. Int.*, *179*, 670–682, doi:10.1111/j.1365-246X.2008.04029.x.

Kendall, R. A., J. X. Mitrovica, and G. A. Milne (2005), On postglacial sea level: II. Numerical formulation and comparative results on spherically symmetric models, *Geophys. J. Int.*, *161*, 679–706, doi:10.1111/j.1365-246X.2005.02553.x.

Larsen, C. F., K. A. Echelmeyer, J. T. Freymueller, and R. J. Motyka (2003), Tide gauge records of uplift along the northern pacific-north american plate boundary, 1937 to 2001, *J. Geophys. Res.*, *108*(B4), 2216, doi:10.1029/2001JB001685.

Larsen, C. F., R. J. Motyka, J. T. Freymueller, K. A. Echelmeyer, and E. R. Ivans (2005), Rapid viscoelastic uplift in southeast Alaska caused by post-Little Ice Age glacial retreats, *Earth Planet. Sci. Lett.*, *237*, 548–560.

Larsen, C. F., R. J. Motyka, A. A. Arendt, K. A. Echelmeyer, and P. E. Geissler (2007), Glacier changes in southeast Alaska and northwest British Columbia and contribution to sea level rise, *J. Geophys. Res.*, *112*, F01007, doi:10.1029/2006JF000586.

Luthcke, S. B., D. D. Rowlands, F. G. Lemoine, S. M. Klosko, D. Chinn, and J. J. McCarthy (2006), Monthly spherical harmonic gravity field solutions determined from GRACE inter-satellite range-rate data alone, *Geophys. Res. Lett.*, *33*, L02402, doi:10.1029/2005GL024846.

Luthcke, S. B., A. A. Arendt, D. D. Rowlands, J. J. McCarthy, and C. F. Larsen (2008), Recent glacier mass changes in the Gulf of Alaska region from GRACE mascon solutions, *J. Glaciol.*, *54*(188), 767–777.

Mitrovica, J. X., and W. R. Peltier (1991), On postglacial geoid subsidence over the equatorial oceans, *J. Geophys. Res.*, *96*(B12), 20,053–20,071.

Mitrovica, J. X., J. Wahr, I. Matsuyama, and A. Paulson (2005), The rotational stability of an ice-age earth, *Geophys. J. Int.*, *161*, 491–506, doi:10.1111/j.1365-246X.2005.02609.x.

Nakiboglu, S., and K. Lambeck (1991), Secular sea-level change, in *Glacial Isostasy, Sea-Level and Mantle Rheology*, edited by R. Sabadini, K. Lambeck, and E. Boschi, pp. 237–258, Kluwer Acad., Dordrecht, Netherlands.

Peltier, W. R. (2004), Global glacial isostasy and the surface of the Ice-Age Earth: The ICE-5G (VM2) model and GRACE, *Annu. Rev. Earth Planet. Sci.*, *32*, 111–149.

Quinn, K., and R. M. Ponte (2010), Uncertainty in ocean mass trends from GRACE, *Geophys. J. Int.*, *181*, 762–768, doi:10.1111/j.1365-246X.2010.04508.x.

Rowlands, D. D., R. D. Ray, D. S. Chinn, and F. G. Lemoine (2002), Short-arc analysis of intersatellite tracking data in a gravity mapping mission, *J. Geod.*, *76*(6–7), 307–316.

Rowlands, D. D., S. B. Luthcke, J. J. McCarthy, S. M. Klosko, D. S. Chinn, F. G. Lemoine, J.-P. Boy, and T. J. Sabaka (2010), Global mass flux solutions from GRACE: A comparison of parameter estimation strategies—Mass concentrations versus Stokes coefficients, *J. Geophys. Res.*, *115*, B01403, doi:10.1029/2009JB006546.

Sneeuw, N. (1994), Global spherical harmonic analysis by least-squares and numerical quadrature methods in historical perspective, *Geophys. J. Int.*, *188*, 707–716, doi:10.1111/j.1365-246X.1994.tb03995.x.

Suito, H., and J. T. Freymueller (2009), A viscoelastic and afterslip post-seismic deformation model for the 1964 Alaska earthquake, *J. Geophys. Res.*, *114*, B11404, doi:10.1029/2008JB005954.

Swenson, S., and J. Wahr (2002), Methods for inferring regional surface-mass anomalies from Gravity Recovery and Climate Experiment (GRACE) measurements of time-variable gravity, *J. Geophys. Res.*, *107*(B9), 2193, doi:10.1029/2001JB000576.

Swenson, S., and J. Wahr (2006), Post-processing removal of correlated errors in GRACE data, *Geophys. Res. Lett.*, *33*, L08402, doi:10.1029/2005GL025285.

Tamisiea, M. E., J. X. Mitrovica, and J. L. Davis (2003), A method for detecting rapid mass flux of small glaciers using local sea level variations, *Earth Planet. Sci. Lett.*, *213*, 477–485.

Tamisiea, M. E., E. W. Leuliette, J. L. Davis, and J. X. Mitrovica (2005), Constraining hydrological and cryospheric mass flux in southeastern Alaska using space-based gravity measurements, *Geophys. Res. Lett.*, *32*, L20501, doi:10.1029/2005GL023961.

Tamisiea, M. E., E. M. Hill, R. M. Ponte, J. L. Davis, I. Velicogna, and N. T. Vinogradova (2010), Impact of self-attraction and loading on the annual cycle in sea level, *J. Geophys. Res.*, *115*, C07004, doi:10.1029/2009JC005687.

Vinogradova, N. T., R. M. Ponte, M. E. Tamisiea, J. L. Davis, and E. M. Hill (2010), Effects of self-attraction and loading on annual variations of ocean bottom pressure, *J. Geophys. Res.*, *115*, C06025, doi:10.1029/2009JC005783.

Wahr, J., M. Molenaar, and F. Bryan (1998), Time variability of the Earth's gravity field: Hydrological and oceanic effects and their possible detection using GRACE, *J. Geophys. Res.*, *103*(B12), 30,205–30,229.

Werner, R. A., and D. J. Scheeres (1997), Exterior gravitation of a polyhedron derived and compared with harmonic and mascon gravitation representations of asteroid 4769 castalia, *Celestial Mech. Dyn. Astron.*, *65*, 313–344.

Wessel, P., and W. H. F. Smith (1998), New, improved version of the generic mapping tools released, *Eos Trans. AGU*, *79*(45), 579.

Zweck, C., J. T. Freymueller, and S. C. Cohen (2002), Three-dimensional elastic dislocation modeling of the postseismic response to the 1964 Alaska earthquake, *J. Geophys. Res.*, *107*(B4), 2064, doi:10.1029/2001JB000409.

J. L. Davis, Lamont-Doherty Earth Observatory, Earth Institute at Columbia University, Palisades, NY 10964, USA. (jdavis@ldeo.columbia.edu)

E. M. Hill, Earth Observatory of Singapore, Nanyang Technological University, 50 Nanyang Ave., N2-01a-15, Singapore 639798. (ehill@ntu.edu.sg)

R. M. Ponte and N. T. Vinogradova, Atmospheric and Environmental Research, Inc., 131 Hartwell Ave., Lexington, MA 02421, USA. (rponte@aer.com; nvinogra@aer.com)

M. E. Tamisiea, National Oceanography Centre, Joseph Proudman Bldg., 6 Brownlow St., Liverpool L3 5DA, UK. (mtam@noc.ac.uk)